Supplementary Material

Electrochemical dual-aptamer biosensor based on nanostructured multielectrode arrays for the detection of neuronal biomarkers

Yuting Zhang[a,b], Gabriela Figueroa-Miranda[a,b], Changtong Wu[a,b], Dieter Willbold[c,d], Andreas Offenhäusser[a,b], Dirk Mayer[a]*

[a]Institute of Biological Information Processing, Bioelectronics (IBI-3), Forschungszentrum Jülich GmbH, 52428 Jülich, Germany

[b]Faculty I, RWTH Aachen, 52062 Aachen, Germany

[c]Institute of Complex Systems (ICS-6), Forschungszentrum Jülich GmbH, 52428 Jülich, Germany

[d]Institut für Physikalische Biologie, Heinrich-Heine-Universität Düsseldorf, 40225 Düsseldorf, Germany

E-mail addresses: dirk.mayer@fz-juelich.de (D. Mayer).

Multielectrode arrays preparation and cleaning

Multielectrode arrays (MEAs) were produced in an ISO 1-3 cleanroom on a borosilicate wafer with a thickness of 500 µm and a diameter of 100 mm, shown in Fig. S1. Firstly, the wafer was spin-coated by a double resist system LOR 3b (Microchem, Newton, MA) and nLOF2070 (MicroChemicals, Ulm, Germany). The feedlines and the 64 microelectrodes pattern were defined via standard photolithography and followed by electron-beam deposition of 10 nm Ti and 200 nm Au, respectively (Pfeiffer PLS 570, Pfeiffer Vacuum, Asslar, Germany). Then, a sonication assisted lift-off step was performed in acetone to remove the photoresist layers. In order to insulate the feedlines, a polyamide (PI) passivation layer was spin-coated onto the wafer. The electrodes and contact pads were directly opened by photolithography with a mask determining their size. Finally, the wafer was diced into individual 24 × 24 mm^2 chips (9 chips/wafer) for further use. For cleaning, new MEAs chips were firstly placed in a chip holder and sonicated in acetone, isopropanol, and Milli-Q water for 5 min, respectively. Then a glass ring with a height of 5 mm and a diameter of 20 mm was adhered to the center of the cleaned chip as a reservoir by a mixture of PDMS and curing agent, Fig. S2. An oxygen plasma oven (Diener Electronic, Germany) was used for MEAs chip cleaning at an O_2 pressure of 0.5 mbar, 50% power, with duration of 3 min.

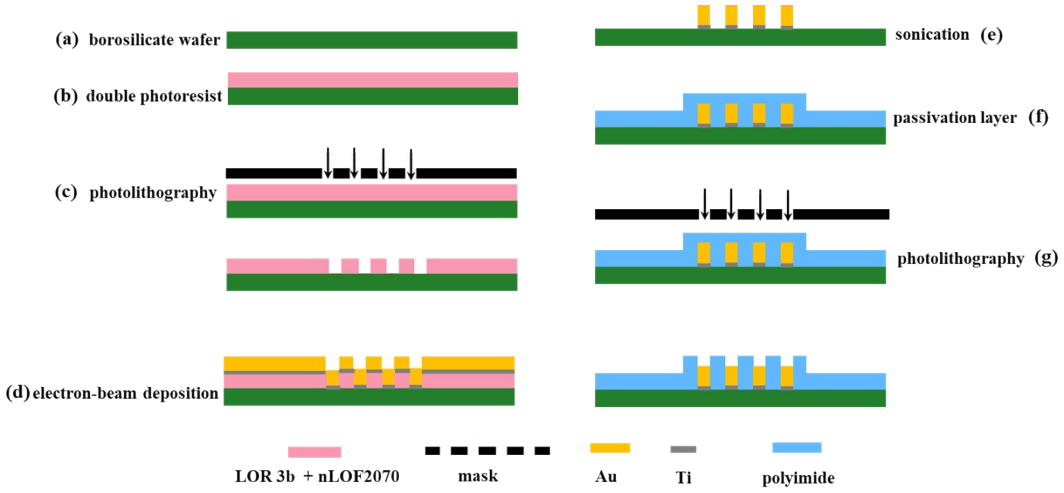

Fig. S1 Fabrication process of multielectrode arrays: (a–b) spin-coating of photoresists; (c) photolithography patterning of gold electrodes; (d) electron-beam deposition of Ti and Au; (d–e) lift-off process assisted by sonication; (f) spin-coating of polyimide for insulating the feedlines; (g) defining the electrode openings and contact pads by photolithography.

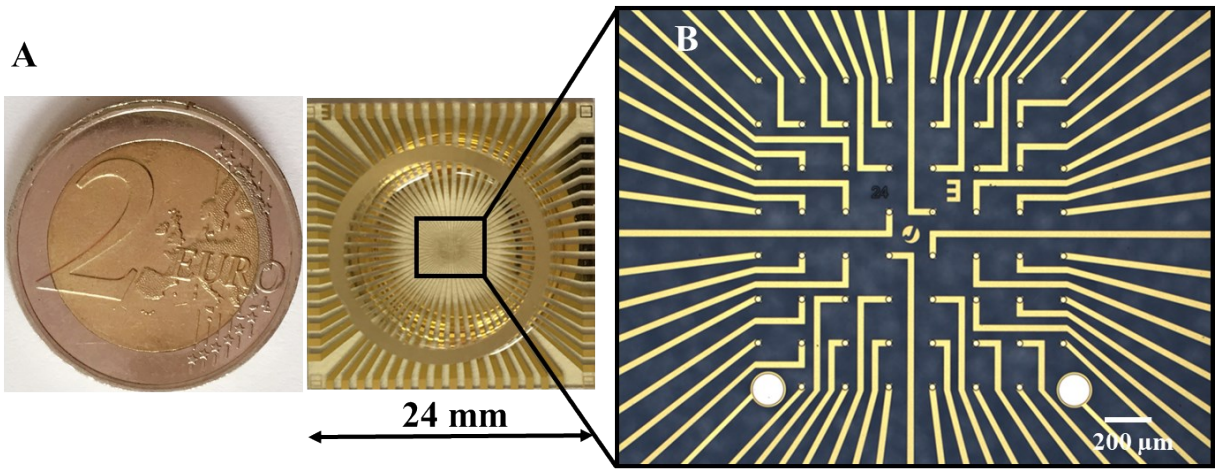

Fig. S2 (A) Borosilicate / gold MEAs with glass ring as electrochemical reservoir cell; (B) central part of the chip with gold feedlines and 64 microelectrodes.

Optimize aptasensor parameters

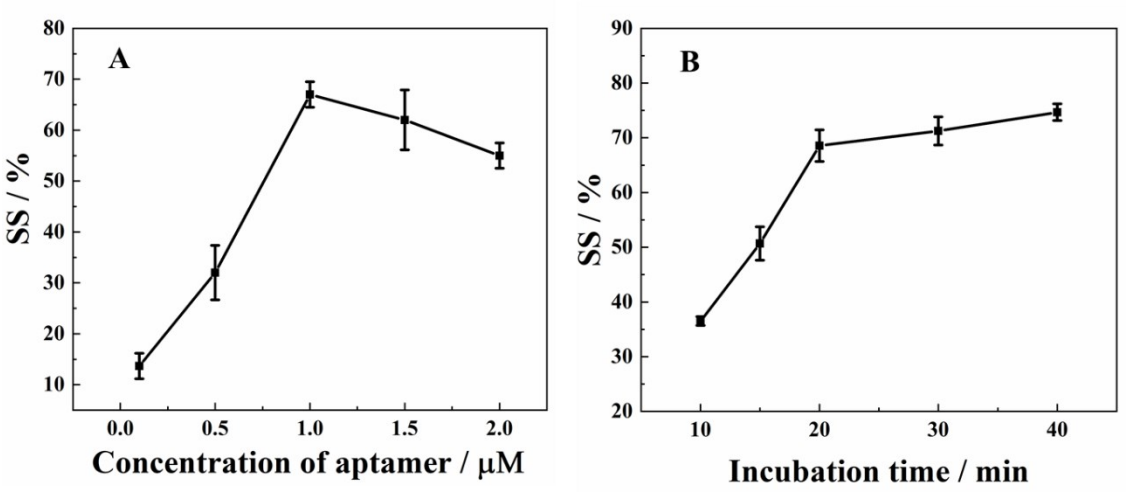

Fig. S3 Effects of aptamer concentration (A) and AβO incubation time (B) on the sensor signal for the detection of 1 nM AβO in 10 mM Tris-HCl + 150 mM NaCl + 5 mM KCl.

Table S1 Performance comparison of the proposed electrochemical aptasensor with other AβO sensors.

Method	Linear range	Detection limit	Ref.
ELISA	12.5 pg/mL – 200 pg/mL	10.7 pg/mL	1
Fluorescent aptsensor	0 μM– 19.25 μM	3.57 nM	2
Electrochemical biosensor	20 pM – 100 nM	8 pM	3
Upconversion fluorescent	0.2 nM – 15 nM	36 pM	4
Peptide-linked immunosorbent assay	0.35 pM − 1.5 pM	-	5
Electrochemiluminescence	0.1 ng/mL − 10 ng/mL	19.95 fg/mL	6
Aptasensor based on 3D-GME	1 pM − 200 nM (10 pg/mL −2 μg/mL)	0.3 pM 3 pg/mL	This work

The regeneration of MEA electrodes by O_2 plasma cleaning

Another approach to regenerate the MEA electrodes is an O_2 plasma cleaning, which however acts globally on all microelectrodes of the chip. Here, a protocol of 0.5 mbar O_2 pressure, 50% power, and an etching time of 3 minutes was used to remove the molecules with sulfhydryl groups from the 3D-GMEs. After O_2 plasma cleaning, soaking in ethanol is required to reduce the oxide layer which formed during the plasma cleaning.[7] After O_2 plasma cleaning and ethanol soaking for 20 minutes, the regenerated microelectrode recovered the original surface mostly, Fig. 5B. A minor increase in the surface area can be noticed presumably caused by a slight degeneration of the electrode passivation. However, the 3D structure was not significantly altered by the O_2 plasma treatment. Consequently, both cleaning methods are suitable for 3D-GME cleaning. The O_2 plasma can be used to regenerate the entire 3D-GME arrays after usage to reset it for a second application. The electrochemical reactivation in NaOH and H_2SO_4 can selectively regenerate individual microelectrodes due to the ability to apply the potential only to a specific electrode, which is crucial for multiple receptor modification and multiple target detection.

Table S2 Performance comparison of the proposed electrochemical aptasensor based on 3D-GMEAs with other ATP sensors.

Method	Linear range	Detection limit	Ref.
Electrochemical current rectification	0–5 μM	114 nM	8
Biosensor on microelectrodes	0.25 μM – 4 μM	9.9 nM	9
Biosensor on MB aptamer	0.1 μM – 50 μM	0.05 μM	10
Fluorescent sensor	–	5 μM	11
Fluorescence resonance energy transfer assay	2 μM – 16 μM	1.7 μM	12
HPLC	1 μM – 12 μM	–	13
Aptamer sensor	1 μM – 1000 μM	1 μM	14
Aptasensor using IOECTs	0.1 nM and 100 nM	0.01 nM	15
Aptasensor based on 3D-GME	0.01 nM – 1000 nM	0.002 nM	This report

Simultaneous detection of AβO and ATP in aCSF

In order to prove that the developed dual-aptasensor platform can selectively detect two targets when they coexist in the sample solution, the dual-aptasensor was first challenged with the non-binding target and subsequently with the matching target. After adding 10 nM ATP to the sample solution, the ACV curve of the AβO aptamer modified 3D-GME did not exhibit a significant current reduction, Fig. S4A. However, after adding 10 nM AβO, the current signal decreased sharply, which indicated that the presence of ATP did not affect the specificity of AβO detection. For ATP aptamer modified 3D-GME, similar observations were made such that the addition of AβO did not alter the ACV current while the subsequent administration of ATP causes a considerable on-signal response, Fig. S4B.

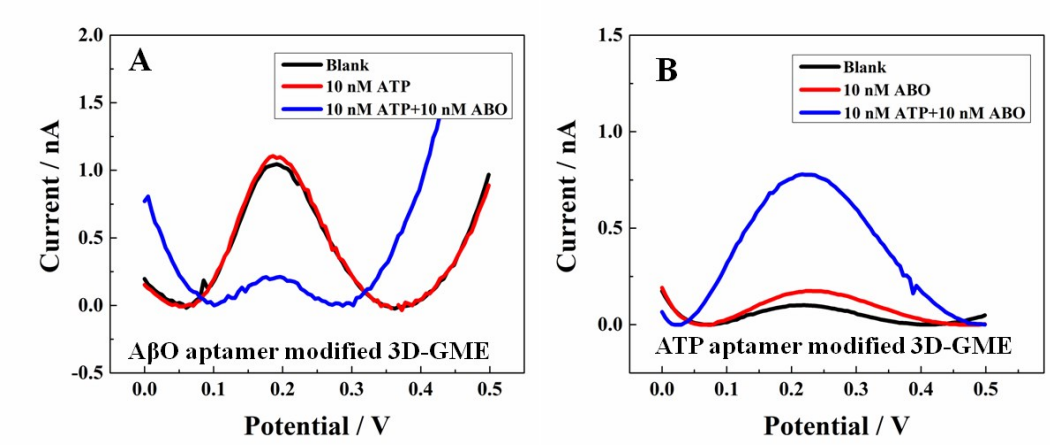

Fig. S4 (A) ACV curves obtained from AβO aptamer modified 3D-GMEs before (black line) and after adding firstly 10 nM ATP (red line) and secondly 10 nM AβO (blue line); (B) ACV curves obtained from ATP aptamer modified 3D-GMEs before (black line) and after adding firstly10 nM AβO (red line), and secondly 10 nM ATP (blue line).

References

1. J. A. Kim, M. Kim, S. M. Kang, K. T. Lim, T. S. Kim and J. Y. Kang, *Biosensors and Bioelectronics*, 2015, **67**, 724-732.
2. L. Zhu, J. Zhang, F. Wang, Y. Wang, L. Lu, C. Feng, Z. Xu and W. Zhang, *Biosensors and Bioelectronics*, 2016, **78**, 206-212.
3. N. Xia, X. Wang, B. Zhou, Y. Wu, W. Mao and L. Liu, *ACS applied materials & interfaces*, 2016, **8**, 19303-19311.
4. L.-F. Jiang, B.-C. Chen, B. Chen, X.-J. Li, H.-L. Liao, H.-M. Huang, Z.-J. Guo, W.-Y. Zhang and L. Wu, *Talanta*, 2017, **170**, 350-357.
5. E. G. Matveeva, J. R. Moll, M. M. Khan, R. B. Thompson and R. O. Cliff, *ACS chemical neuroscience*, 2017, **8**, 1213-1221.
6. Y. Jia, L. Yang, R. Feng, H. Ma, D. Fan, T. Yan, R. Feng, B. Du and Q. Wei, *ACS applied materials & interfaces*, 2019, **11**, 7157-7163.
7. S. Gandhi and A. Y. Abramov, *Oxidative medicine and cellular longevity*, 2012, **2012**.
8. L. Feng, A. Sivanesan, Z. Lyu, A. Offenhäusser and D. Mayer, *Biosensors and bioelectronics*, 2015, **66**, 62-68.
9. B. A. Patel, M. Rogers, T. Wieder, D. O'Hare and M. G. Boutelle, *Biosensors and Bioelectronics*, 2011, **26**, 2890-2896.
10. Y. Wang, X. He, K. Wang and X. Ni, *Biosensors and Bioelectronics*, 2010, **25**, 2101-2106.
11. H.-Z. He, V. P.-Y. Ma, K.-H. Leung, D. S.-H. Chan, H. Yang, Z. Cheng, C.-H. Leung and D.-L. Ma, *Analyst*, 2012, **137**, 1538-1540.
12. X. He, Z. Li, X. Jia, K. Wang and J. Yin, *Talanta*, 2013, **111**, 105-110.
13. M. von Papen, S. Gambaryan, C. Schuetz and J. Geiger, *Transfusion Medicine and Hemotherapy*, 2013, **40**, 109-116.
14. F. Liu, J. Zhang, R. Chen, L. Chen and L. Deng, *Chemistry & biodiversity*, 2011, **8**, 311-316.
15. Y. Liang, C. Wu, G. Figueroa-Miranda, A. Offenhäusser, D. Mayer, *Biosensors and Bioelectronics*, 2019, **144**, 111668.